Supporting information for:

Low-Spin Ferriheme Models of the Cytochromes: Mössbauer Spectra of Six Crystalline Complexes Having Axial Ligand Plane Dihedral Angles Ranging from 0^o to 90^o

Thomas Teschner,[‡] Liliya Yatsunyk,[†] Volker Schünemann,[‡] Hauke Paulsen,[‡] Heiner Winkler,[‡] Chuanjiang Hu,[#] W. Robert Scheidt,[#] F. Ann Walker,[†] and Alfred X. Trautwein*[‡]

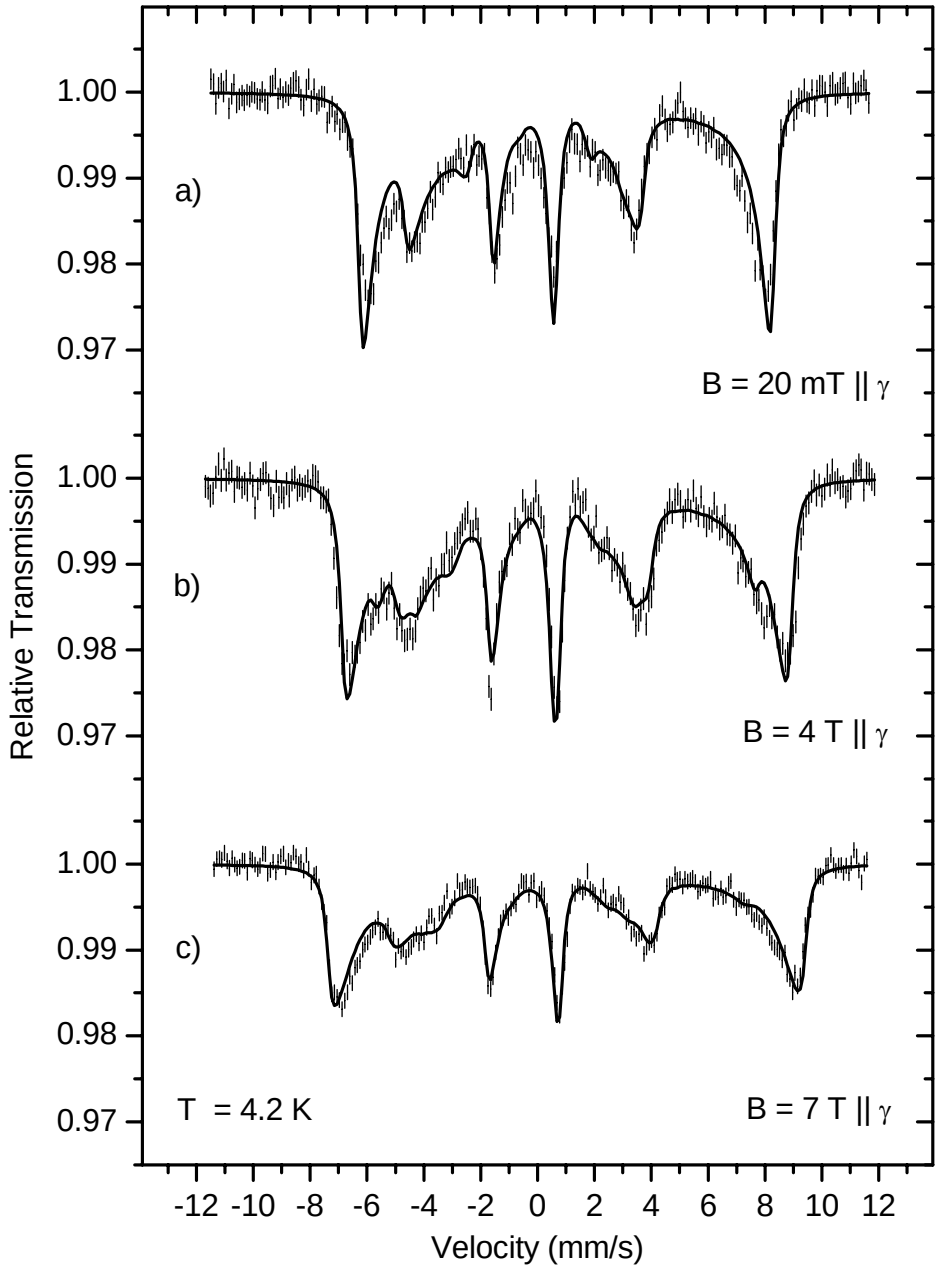

Figure S1. Mössbauer spectra of *perp*-[(OMTPP)Fe(1-MeIm)$_2$]Cl ($\Delta\varphi = 90°$) obtained at 4.2 K in the presence of several different magnetic fields applied parallel to the γ-beam (20 mT (a), 4 T (b), and 7 T (c)). The solid lines are fits performed in the limit of *slow relaxation* with parameters given in Table 1.

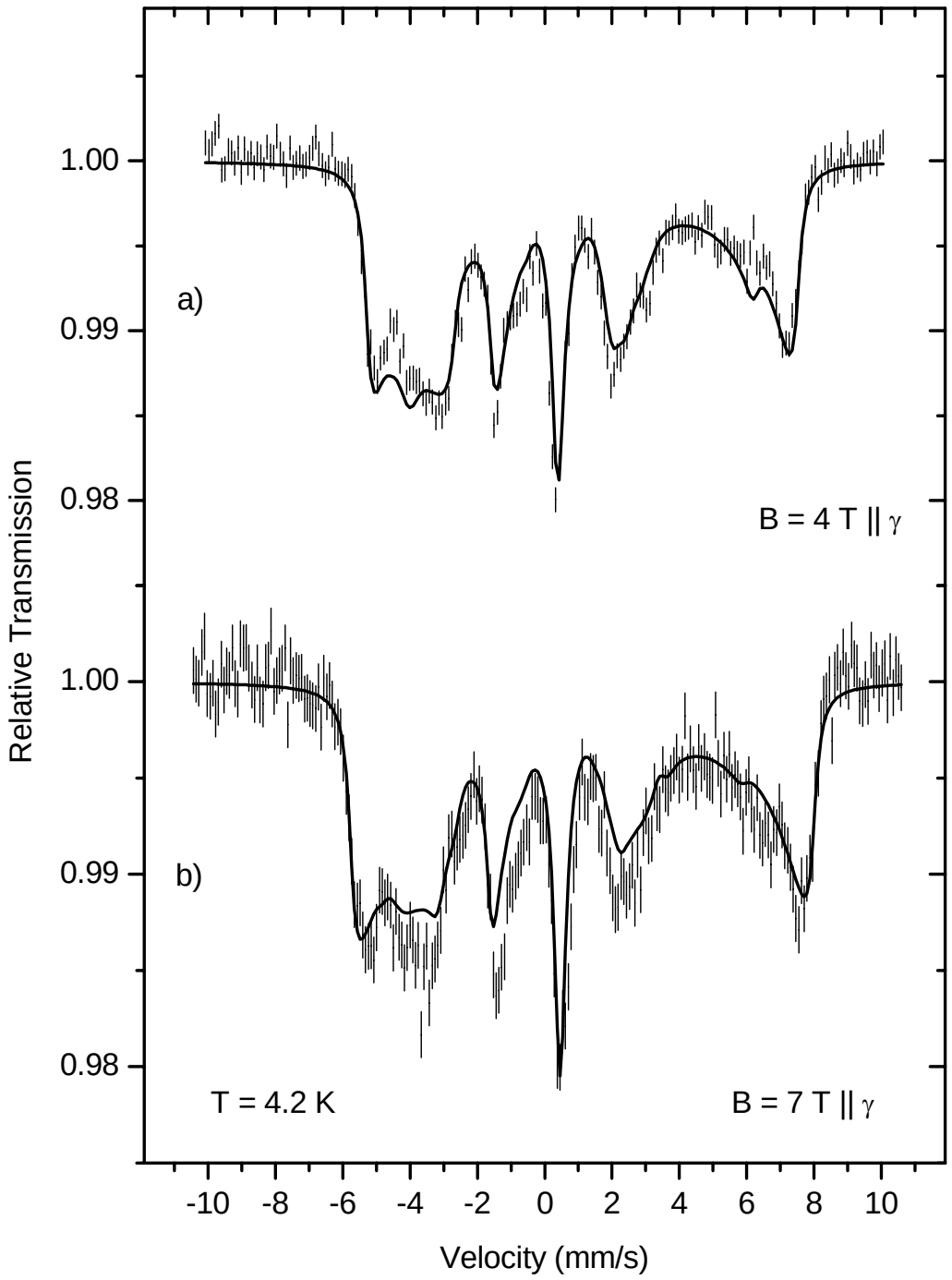

Figure S2. Mössbauer spectra of *perp*-[(OETPP)Fe(1-MeIm)$_2$]Cl ($\Delta\varphi = 73.1°$) recorded at 4.2 K in the presence of two different magnetic fields applied parallel to the γ-beam (4 T (a), and 7 T (b)). The solid lines are fits performed in the limit of *slow relaxation* with parameters given in Table 1.

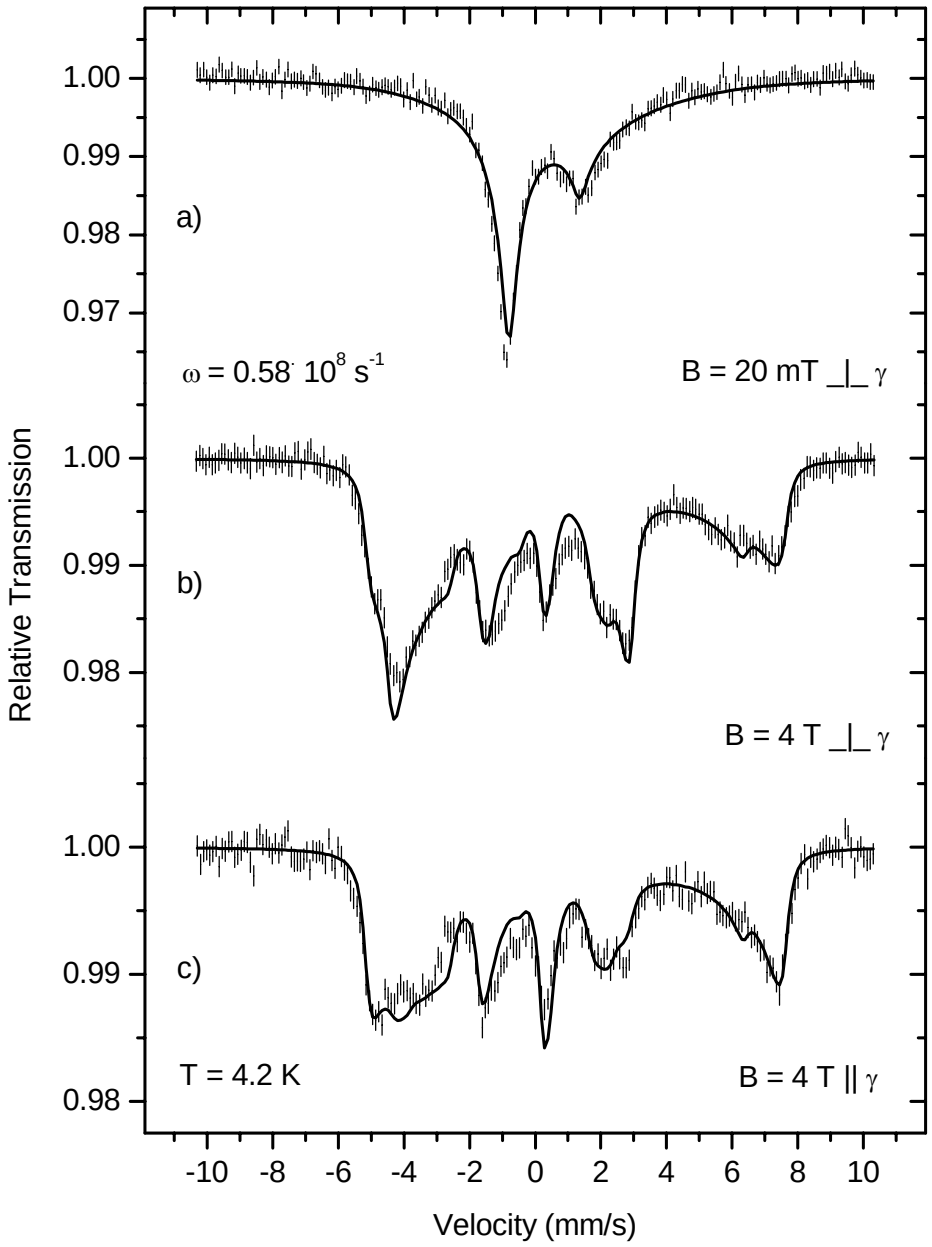

Figure S3. Mössbauer spectra of [(OETPP)Fe(4-Me_2NPy)$_2$]Cl ($\Delta\varphi = 70°$) taken at 4.2 K in the presence of two different magnetic fields applied perpendicular (20 mT (a), and 4 T (b)) and parallel (4 T (c)) to the γ-beam. The solid line in the spectrum recorded at 20 mT (a) is a fit taking *spin-spin relaxation effects* (with relaxation rate ω as indicated) into account[75] and the other solid lines (4 (b) and (c)) are fits performed in the limit of *slow relaxation* with parameters given in Table 1.

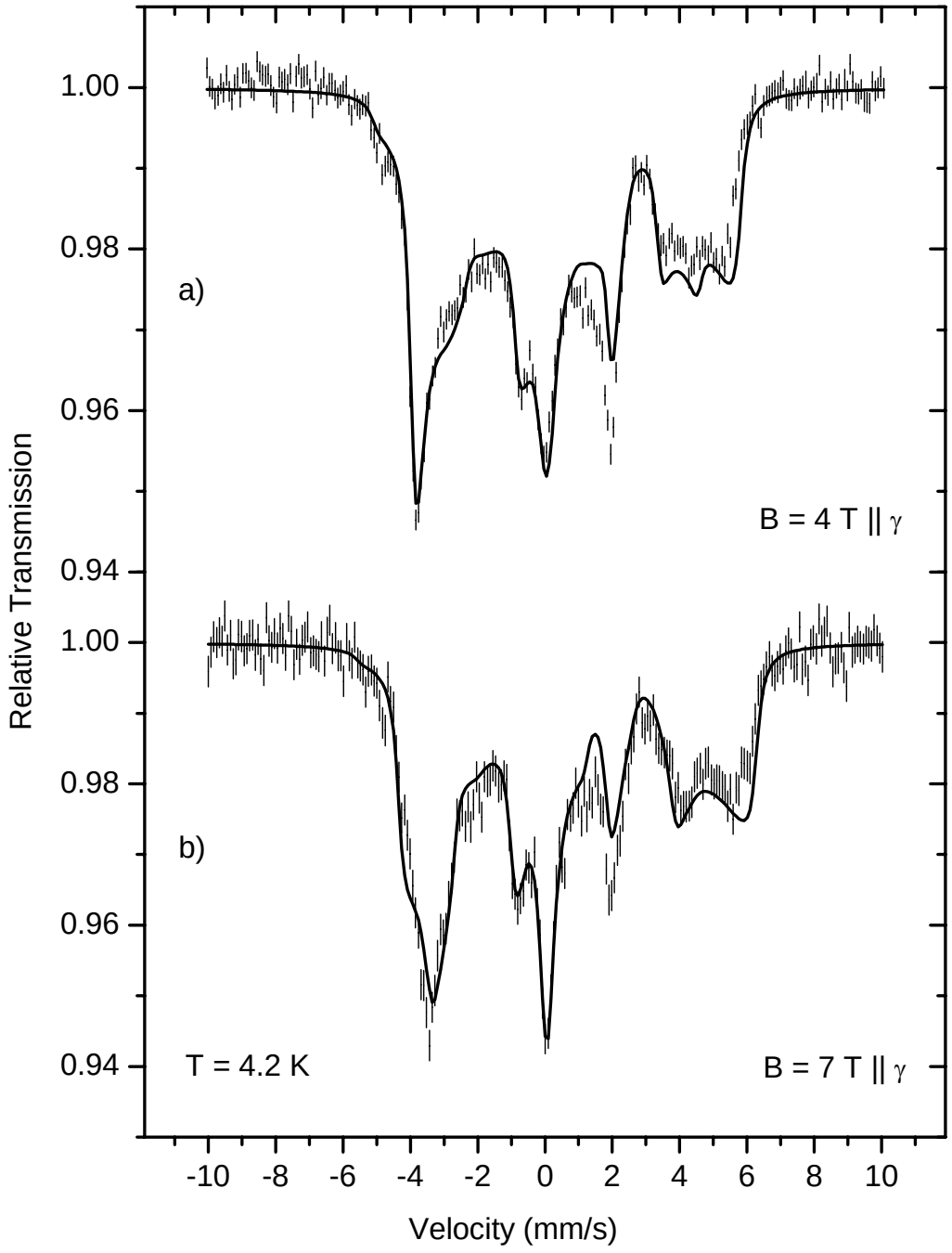

Figure S4. Mössbauer spectra of *paral*-[(TMP)Fe(5-MeHIm)$_2$]ClO$_4$ ($\Delta\varphi = 26^{o},30°$)[70] at 4.2 K obtained in the presence of two different magnetic fields applied parallel to the γ-beam (4 T (a), and 7 T (b)). The solid lines are fits performed in the limit of *slow relaxation* with parameters given in Table 1.

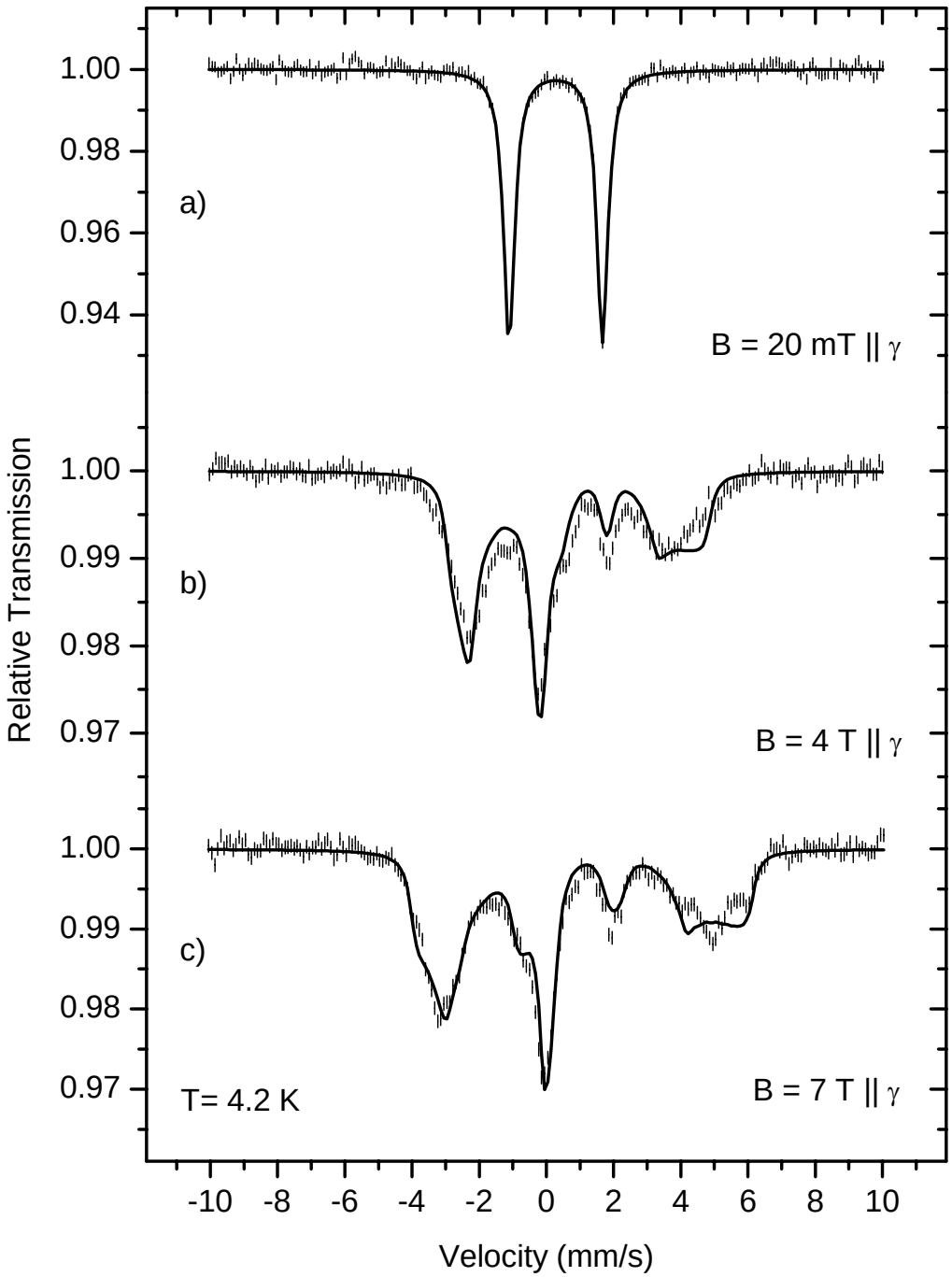

Figure S5. Mössbauer spectra of *paral*-[(OMTPP)Fe(1-MeIm)$_2$]Cl ($\Delta\varphi$ = 19.5°) recorded at 4.2 K in the presence of several different magnetic fields applied parallel to the γ-beam (20 mT (a), 4 T (b), and 7 T (c)). The solid lines are fits performed in the limit of *fast relaxation* with parameters given in Table 1.

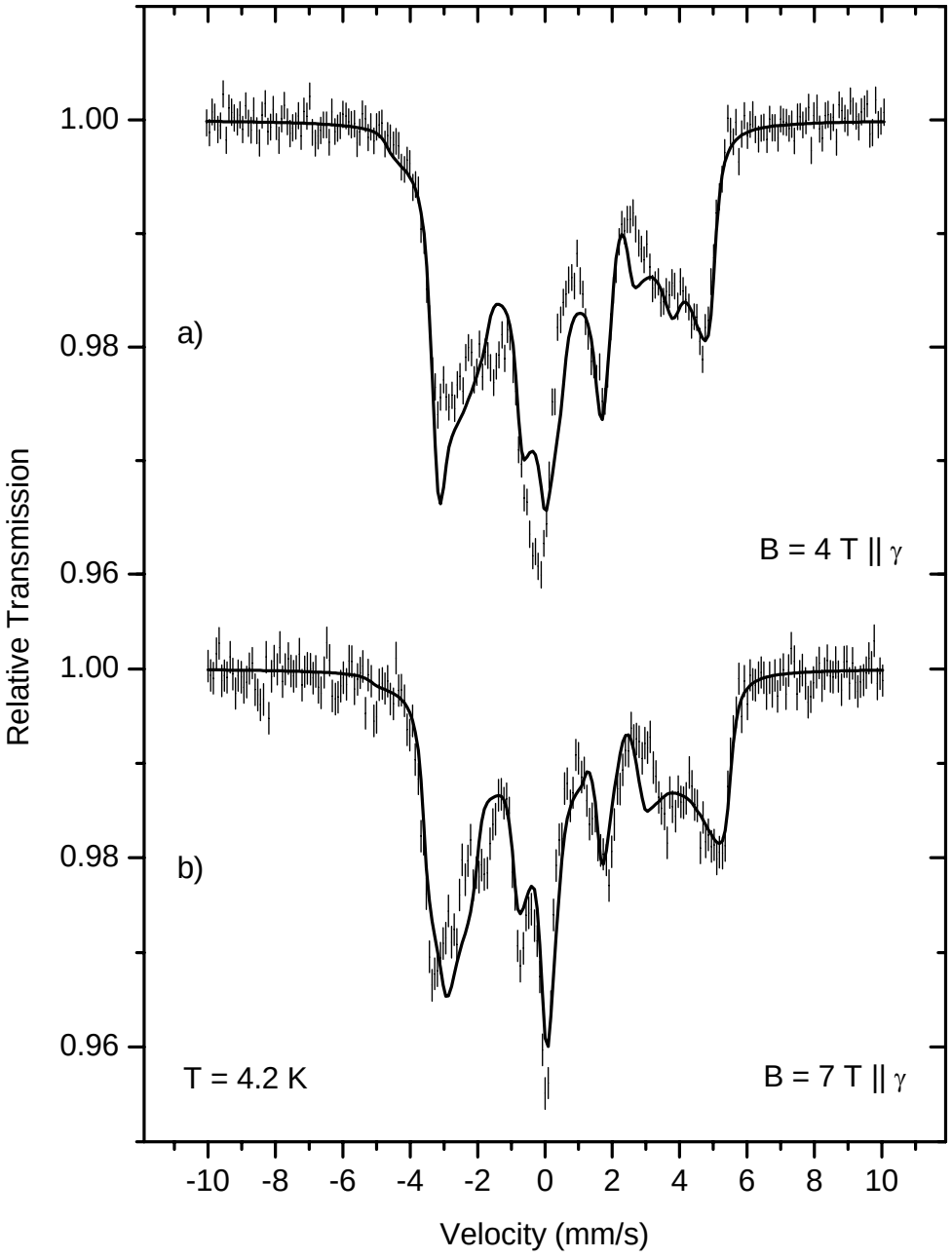

Figure S6. Mössbauer spectra of $[(TMP)Fe(ImH)_2]ClO_4$ ($\Delta\varphi = 0°$) obtained at 4.2 K in the presence of two different magnetic fields applied parallel to the γ-beam (4 T (a) and 7 T (b)). The solid lines are fits performed in the limit of *slow relaxation* with parameters given in Table 1.

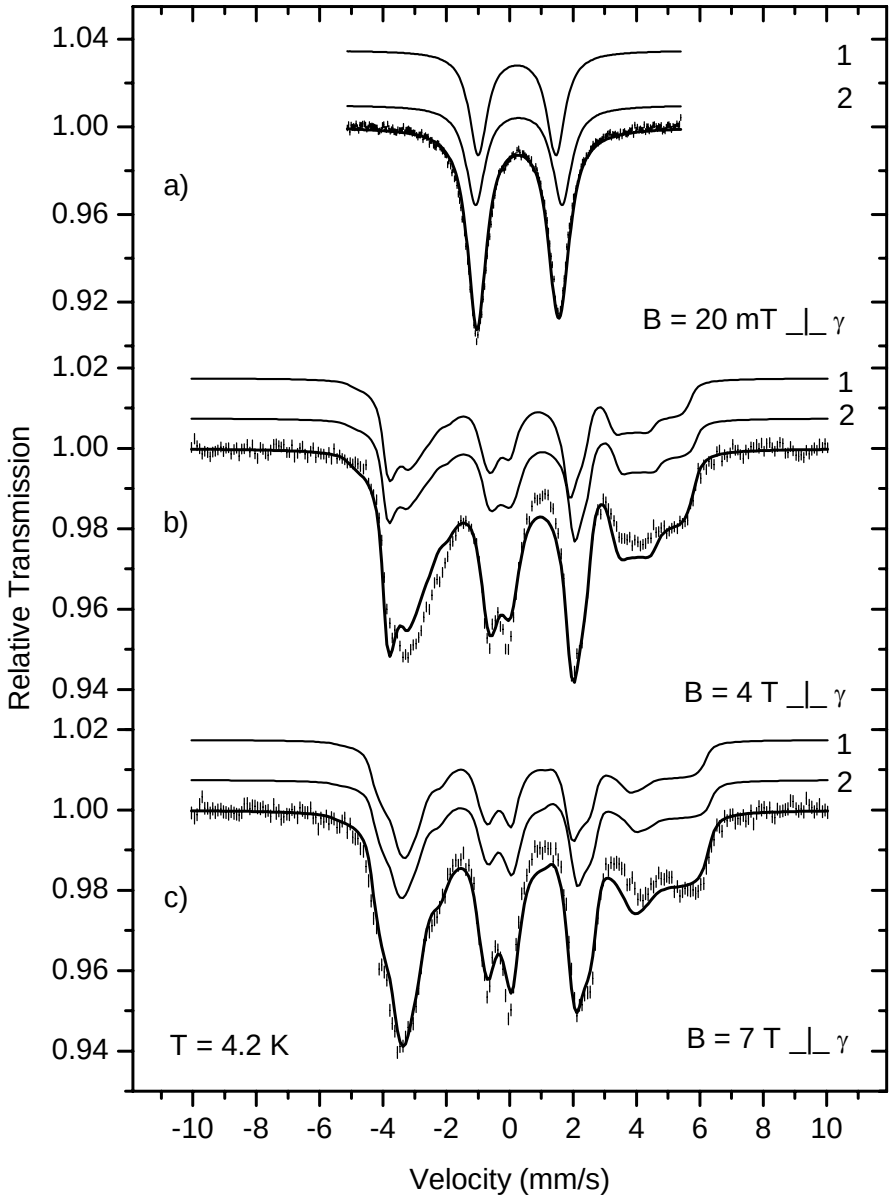

Figure S7. Mössbauer spectra of *paral*-$[(TMP)Fe(5\text{-}MeHIm)_2]^+$ ($\Delta\varphi = 26^o$ and 30^o) obtained at T = 4.2 K in magnetic fields (20 mT (a), 4 T (b) and 7 T (c) as indicated perpendicular to the γ-beam. The solid line in (a) is a Lorentzian fit and the others are fits performed in the limit of *slow relaxation* with parameters given in the table below.

δ_1 (mm/s)	ΔE_{Q1} (mm/s)	δ_2 (mm/s)	ΔE_{Q2} (mm/s)	η	$A/g_N\mu_N$ (kG)
0.29	2.73	0.32	2.45	–2.22	(–426, 198, 487)

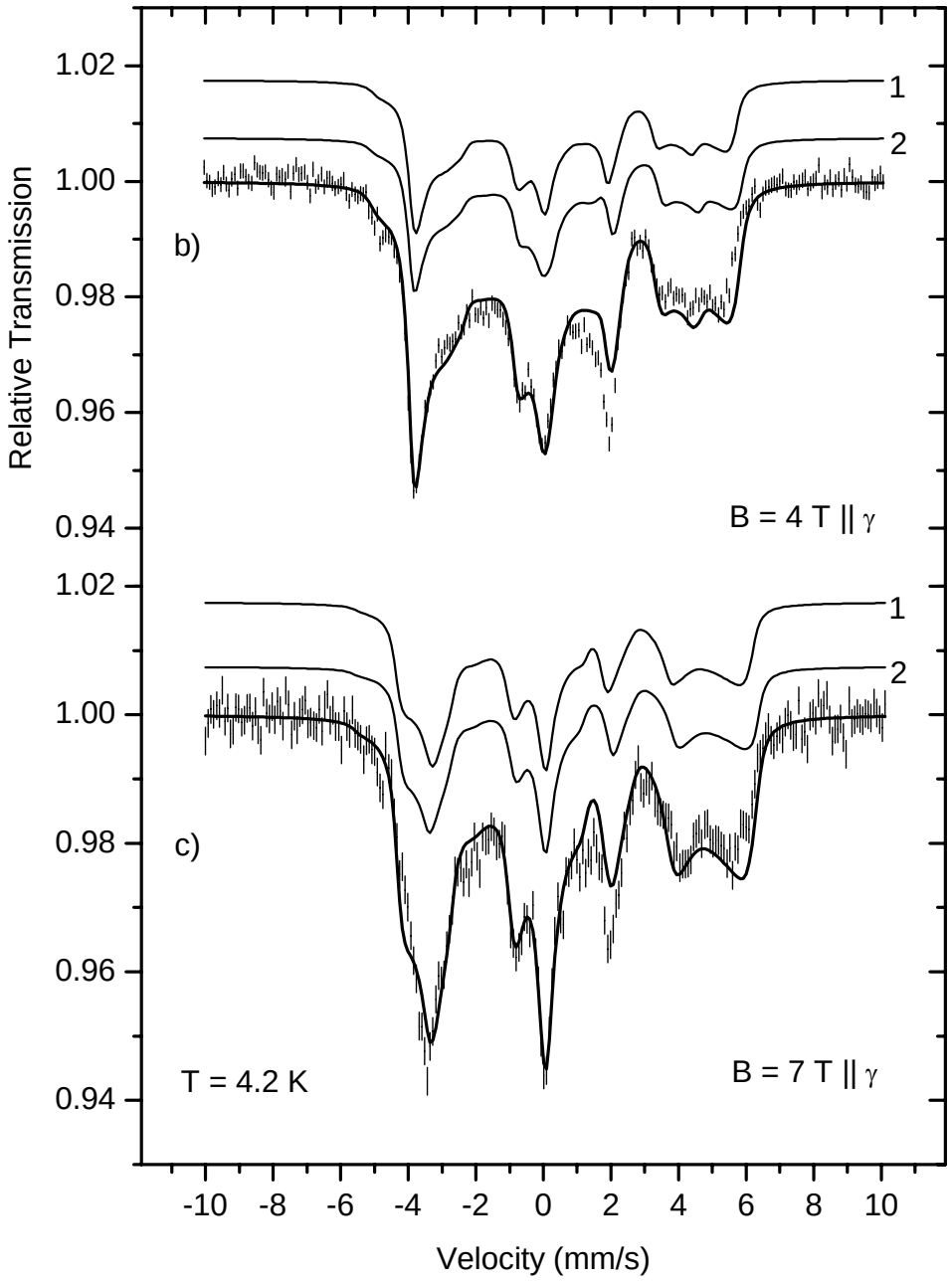

Figure S8. Mössbauer spectra of *paral*-[(TMP)Fe(5-MeHIm)$_2$]$^+$ ($\Delta\varphi = 26^o$ and 30^o) obtained at T = 4.2 K in magnetic fields (20 mT (a), 4 T (b) and 7 T (c) as indicated parallel to the γ-beam. The solid line in (a) is a Lorentzian fit and the others are fits performed in the limit of *slow relaxation* with parameters given in the table below.

δ_1 (mm/s)	ΔE_{Q1} (mm/s)	δ_2 (mm/s)	ΔE_{Q2} (mm/s)	η	$A/g_N\mu_N$ (kG)
0.29	2.73	0.32	2.45	–2.22	(–426, 198, 487)

Table S1. Number and Distances of Nearest Iron-Iron Neighbors in the Complexes of this Study.

Complex	Space Group	Number of Fe-Fe neighbors	Distance, Å	Appearance of 4.2 K 20 mT Mössbauer spectrum	Relaxation rate ω (s^{-1})
paral-[(OMTPP)Fe(1-MeIm)$_2$]Cl ($\Delta\varphi = 19.5^o$)	*Pc*	2 2 2	9.54 10.128 12.15	sharp doublet	Fast
paral-[(TMP)Fe(5-MeHIm)$_2$]ClO_4 ($\Delta\varphi = 26^o, 30^o$)[70]	*P2$_1$*	2 2 4	10.67 11.897 13.651	asymmetric doublet (two sharp doublets)	1.42×10^8 (Fast)[a]
[(TMP)Fe(1-MeIm)$_2$]ClO_4 ($\Delta\varphi = 0^o$)	$P\bar{1}$	2 2 2	10.409 12.061 13.603	asymmetric doublet (two sharp doublets)	0.81×10^8 (Fast)[a]
[(OETPP)Fe(4-Me$_2$NPy)$_2$]Cl ($\Delta\varphi = 70^o$)	*Pna2(1)*	2 2 4	12.245 13.651 14.052	broad asymmetric doublet	0.58×10^8
perp-[(OETPP)Fe(1-MeIm)$_2$]Cl ($\Delta\varphi = 73.1^o$)	*P2$_1$*	2 2 4	12.651 12.86 13.058	broad asymmetric doublet	0.47×10^8
perp-[(OMTPP)Fe(1-MeIm)$_2$]Cl ($\Delta\varphi = 90^o$)	*I-43d*	8 4 8	12.232 14.62 17.9	six-line pattern	Slow

a) Alternative fit (Fig. S7 and S8 for *paral*-[(TMP)Fe(5-MeHIm)$_2$]ClO_4 and similar fits for [(TMP)Fe(1-MeIm)$_2$]ClO_4, not shown) possible because of two slightly different iron sites within the unit cell.

Table S2. Ligand deviations from the normal to the mean porphyrin plane, and ligand plane orientations with respect to the N-Fe-N axes for molecules of this study.[a]

Complex	L_1 Deviation from heme normal, ^{o}	L_1 Orientation with respect to Porph N, ^{o}	L_2 Deviation from heme normal, ^{o}	L_2 Orientation with respect to Porph N, ^{o}	Ref. in text
1 $[(OEP)Fe(4\text{-}Me_2NPy)_2]^+$	0	+36	0	36	42
2 $[(TMP)Fe(1\text{-}MeIm)_2]^+$	6.3 1.2	+23 +41	6.3 1.2	23 41	42
4 *paral*-$[(OMTPP)Fe(1\text{-}MeIm)_2]^+$	9.1	–12.6	3.2	6.9	45
7 *paral*-$[(TMP)Fe(5\text{-}MeHIm)_2]^+$	4.0 6.8	–10 –14	1.7 3.4	20 12	43
8 NP4-histamine	12	+12 (Hm)	10	44 (His)	78
11 $[(OETPP)Fe(4\text{-}Me_2NPy)_2]^+$	12.2	–9.0	0.9	61.0	44
12 $[(OETPP)Fe(1\text{-}MeIm)_2]^+$	3.3	+9.6	2.5	82.7	45
13 $[(TMP)Fe(4\text{-}Me_2NPy)_2]^+$	1.7	–37	7.6	42	42
14 $[(TPP)Fe(2\text{-}MeImH)_2]^+$	10.6	–32	4.3	57	38
15 *perp*-$[(OMTPP)Fe(1\text{-}MeIm)_2]^+$	0	–29.3	0	60.7	45

a) Deviations from the heme normal larger than 9^o are marked in red.